Crowdsourcing-Based Fingerprinting for Indoor Location in Multi-Storey Buildings

RICARDO SANTOS[1,2], **RICARDO LEONARDO**[1,2], **MARÍLIA BARANDAS**[1,2], **DINIS MOREIRA**[1], **TIAGO ROCHA**[1], **PEDRO ALVES**[1], **JOÃO P. OLIVEIRA**[3,4], **AND HUGO GAMBOA**[1,2], (Senior Member, IEEE)

[1]Associação Fraunhofer Portugal Research, 4200-135 Porto, Portugal
[2]Laboratório de Instrumentação, Engenharia Biomédica e Física da Radiação (LIBPhys-UNL), Departamento de Física, Faculdade de Ciências e Tecnologia da Universidade Nova de Lisboa (FCT-UNL), 2829-516 Caparica, Portugal
[3]Information Sciences, Technologies and Architecture Research Center (ISTAR-IUL), Instituto Universitário de Lisboa (ISCTE-IUL), 1649-026 Lisboa, Portugal
[4]Instituto de Telecomunicações (IT), Instituto Superior Técnico (IST), 1049-001 Lisboa, Portugal

Corresponding author: Ricardo Santos (ricardo.santos@fraunhofer.pt)

ABSTRACT The number of available indoor location solutions has been growing, however with insufficient precision, high implementation costs or scalability limitations. As fingerprinting-based methods rely on ubiquitous information in buildings, the need for additional infrastructure is discarded. Still, the time-consuming manual process to acquire fingerprints limits their applicability in most scenarios. This paper proposes an algorithm for the automatic construction of environmental fingerprints on multi-storey buildings, leveraging the information sources available in each scenario. It relies on unlabelled crowdsourced data from users' smartphones. With only the floor plans as input, a demand for most applications, we apply a multimodal approach that joins inertial data, local magnetic field and Wi-Fi signals to construct highly accurate fingerprints. Precise movement estimation is achieved regardless of smartphone usage through Deep Neural Networks, and the transition between floors detected from barometric data. Users' trajectories obtained with Pedestrian Dead Reckoning techniques are partitioned into clusters with Wi-Fi measurements. Straight sections from the same cluster are then compared with subsequence Dynamic Time Warping to search for similarities. From the identified overlapping sections, a particle filter fits each trajectory into the building's floor plans. From all successfully mapped routes, fingerprints labelled with physical locations are finally obtained. Experimental results from an office and a university building show that this solution constructs comparable fingerprints to those acquired manually, thus providing a useful tool for fingerprinting-based solutions automatic setup.

INDEX TERMS Crowdsourcing, fingerprinting, indoor location, inertial tracking, magnetic field, multi-storey, unsupervised, Wi-Fi.

I. INTRODUCTION

Nowadays, the use of Global Positioning System (GPS) has become vulgar and it is around us during our everyday lives. Using a global network of satellites, a user or an object can be located with at least four different satellites through the process of trilateration. This technology has become extremely reliable and accurate, but it does not work inside buildings or underground. This is due to the loss of the satellite signal as it has to go through solid structures, such as walls. To further increase the losses, buildings with metallic structures in their foundations will see an increased decline in signal strength or even total loss due to the Faraday cage effect. This problem can affect potential applications for indoor location such as tracking automated cars inside warehouses, locating patients and visitors in healthcare facilities, keep track of inventory in smart offices, among other applications.

To solve this problem, two major groups of Indoor Positioning Systems (IPS) arose, those that require the installation of additional infrastructure and infrastructure-free solutions.

The associate editor coordinating the review of this manuscript and approving it for publication was Cesar Vargas-Rosales.

The former usually resorts to beacons capable of emitting signals that are received and re-transmitted back. By using similar techniques to trilateration, these methods can locate the receiver. The drawbacks of such solutions are the high costs associated with the installation and maintenance of the required infrastructure, while the main advantage is their higher accuracy [1]–[4].

Regarding the infrastructure-free IPS, the most common type utilises one or more sources of information, such as Wi-Fi and magnetic field signals. These are possible given the embedding of several sensors in smartphones, from Inertial Measurement Units (IMU) to radio antennas. To exploit such information, the most common approach is the use of fingerprints on fingerprinting-based solutions. A fingerprint is the mapping of a building with the desired sources of information, collected by sensors across the area. At the end of the data collection process, after saving to each position the corresponding sensor reading, a map is constructed using the gathered information and a schematic. This fingerprint can be used to compare real-time data with the one in the fingerprint to help locate the user [5]–[7].

As mentioned, most infrastructure-free methods use fingerprints as the basis for storing information. However, they require a time-consuming construction process, as the entire area has to be covered by the sensors.

To avoid this problem, new approaches have been tried and one of the most promising is crowdsourcing. This technique has been used in numerous areas, such as outdoor navigation or collaborative translation. Crowdsourcing is a method to solve complex problems with help from a group of users who, whether actively or opportunistically, assist on simpler tasks [8]. Thus, crowdsourcing comes as a solution to address the initial setup burden of fingerprinting-based IPS [9]. Leveraging the sensing capabilities of smartphones, anonymous users can support the fingerprints construction process.

For this purpose, in an initial phase, crowdsourcing contributors naturally walk over the area of interest while their smartphones' sensors collect data opportunistically. Then, with further processing after the collection campaign, a fingerprint can be built automatically and maintained when buildings change. However, existing algorithms present limitations, either regarding their results, limited application or the need for manual input of a set of parameters.

To address these limitations, we present an innovative approach to automatically construct fingerprints with crowdsourcing, for the desired environmental sources. After the initial data collection campaign, which may be defined according to the use case needs and complemented in later iterations, the construction process can be triggered. Given the floor plans for the different floors, users' trajectories are reconstructed with Pedestrian Dead Reckoning (PDR) and iteratively fitted to the correct locations with a particle filter, aided by a barometer-based module to detect floor transitions. When compared to the literature, the great innovative aspect of our solution is its unique multimodal approach, taken

to enhance the mapping accuracy. Depending on scanning restrictions from users' devices, trajectories are firstly partitioned into Wi-Fi similar areas with an unsupervised Machine Learning (ML) algorithm. Straight segments of the same group and with approximate orientation are compared with an adaptive distance measure based on the perceived magnetic field, to identify overlapping areas with high confidence. With the proper fitting of each route into the correct floor plan from mapped overlaps in previous iterations, fingerprints are obtained. To assert the validity of the proposed solution, evaluation tests were performed in two different settings, a single-floor office building, and a larger multi-storey university, using crowdsourced data from one user left out of the construction process. The crowdsourcing fingerprints were compared to those obtained by the traditional method and the signal differences were computed to verify their similarity. Also, the acquisitions from the test user were submitted to an IPS using both the crowdsourced and traditional fingerprints. The attained results on the test conditions assert the quality of the algorithm.

The innovative aspects of this work for the automatic fingerprints construction based on crowdsourcing are the following:

- Leverage different pervasive sources depending on the use case;
- Improved accuracy through multimodal validation of crowd contributions;
- Accurate step detection based on Deep Learning;
- Mapping of multi-storey buildings from floor transitions detection;
- Unconstrained by buildings dimensions, fitting any indoor environment.

This paper is organised as follows: Section II discusses the literature review and the previous work of our team on this topic. The detailed description of the proposed approach is available in Section III. In Section IV we present and discuss the performance of our solution on the evaluation tests on two distinct environments. At last, in Section V the conclusions are taken and the future directions envisioned.

II. RELATED WORK

Indoor location solutions often rely on fingerprinting techniques to decrease implementation costs related to the acquisition and maintenance of radio equipment. However, such infrastructure-free solutions need the manual labour of acquiring fingerprints, either during the initial setup and whenever the venue's characteristics change. Especially in large environments, this effort may suppress the benefits of fingerprinting-based solutions.

Works have been proposed to address this issue, resorting to crowdsourcing to tackle the labour-intensive fingerprints construction process. Crowdsourcing is thus used in this context to acquire a significant amount of data from large groups of users. Therefore, the need for an expert is dismissed thanks to the participation of ordinary users [10]. Providing

a comparable level of accuracy on fingerprints construction will contribute to decreasing the costs of deployment and maintenance, crucial to widen the usage scenarios of indoor localisation.

Depending on the use case, different approaches to crowdsourcing may be deployed. While in some cases users may need to take active action while participating in the data collection, in others the acquisition may take place opportunistically. As an example, in [11], crowdsourcing users need to annotate when passing by specific landmarks, so the system can use these predetermined positions to adjust the localisation estimations. On the other hand, in [12], users only need to normally walk throughout the venues, while smartphones collect data opportunistically from the available sources, dismissing any further effort from the crowd. When crowdsourcing-based solutions are deployed into production through marketable products, considerations regarding incentive mechanisms and privacy issues must be taken into account to ensure adherence from data collection contributors [10], [13].

Throughout the literature, different approaches relying on the use of crowdsourcing have been considered. Depending on the use-case, different sources of information and processing techniques are leveraged. Furthermore, while some solutions require buildings' floor plans to start fingerprints mapping, others dismiss this requirement, demanding instead additional input parameters.

A. FLOOR PLAN-INDEPENDENT CROWDSOURCING

Some authors ground their efforts on the premise that floor plans are not available in specific contexts, and the manual mapping process may imply prohibitive costs. Therefore, some solutions seek for the mapping process automation [14]–[16], which often rely on inertial sensing to apply on PDR techniques, together with additional sources as the Wi-Fi distribution or local magnetic field.

Other works complement the floor plan mapping process with the further construction of fingerprints for different layers. Li *et al.* [17] leverage users' inertial data, where they split trajectories into segments, the corridors. Magnetic features are retrieved from such segments, which are clustered to identify similar sequences. Collected Wi-Fi measurements are assigned to a final position after obtaining the final corridor map. Luo *et al.* [18] developed PiLoc, a system that constructs Wi-Fi fingerprints by segmenting users' trajectories into sets of curves with adjacent straight sections. The authors find similar curves by evaluating their shape and Wi-Fi trend, which are merged into a final floor plan and fingerprints. With SmartSLAM, Shin *et al.* [19] employ a Simultaneous Localisation and Mapping (SLAM) approach to construct floor plans with Wi-Fi fingerprints based on Hidden Markov Models (HMM), which leverage inertial sensing and Wi-Fi measurements to expand the inferred trajectories.

In a previous approach to this topic, our group proposed in [12] the use of crowdsourcing on an algorithm to construct indoor floor plans and geomagnetic and Wi-Fi fingerprints

effortlessly. The solution leverages inertial sensing to infer crowdsourcing users' trajectories, from which straight segments are retrieved and clustered, to divide venues into areas with similar Wi-Fi pattern. Same cluster segments are compared with an adaptive distance measure to identify which are overlapping. The floor plans are constructed by performing geometric transformations to routes, so similar sections are mapped into the same locations. Finally, fingerprints are retrieved by matching the collected sources into each position.

Although these solutions fit specific use cases where obtaining a floor plan is not feasible, they present lower accuracy due to lacking reference points or map constrains. Furthermore, in most scenarios, a map is necessary to display the localisation information to the systems' users, so they can navigate throughout a mall or an airport, for example.

B. FLOOR PLAN-DEPENDENT CROWDSOURCING

When the venues' floor plans are given, the fingerprints construction process is constrained by the possible locations where users may be, which limits the error possibilities. From crowdsourcing data, different approaches may use floor plans as the only requirement for the fingerprints construction or use them together with additional inputs.

Trogh *et al.* [20] optimise Wi-Fi signal maps with the input of a set of APs' locations, to calculate an initial simulated fingerprint. With new data, radio values are corrected with the Viterbi algorithm, used to estimate the most likely path, considering both the movement information and the similarity between Wi-Fi measurements and preliminary fingerprints. In another approach, Ahn *et al.* [21] use as landmarks the location of payment terminals in a shopping mall, to estimate an initial radio map and correct the users' locations. Then, the authors update the fingerprint with the collected Wi-Fi data while crowdsourcing users walk throughout the building.

With no further inputs, Wu *et al.* developed LiFS [22], a solution that resorts to Multi-Dimensional Scaling (MDS) to create a stress-free floor plan that reflects real walking distances between locations. By evaluating distances between Wi-Fi measurements, the authors measure spatial similarity to obtain their locations and construct the Wi-Fi fingerprints. The floor plan is used by Zhou *et al.* [16] to extract the possible paths that users may take. If in vertexes activities such as turns happen, an activity recognition algorithm is applied, together with users' trajectories inference, to compute the corresponding positions and obtain the Wi-Fi fingerprints. A different approach is taken by Rai *et al.* with Zee [23], where a particle filter is applied to the collected inertial data, to expand the possible positions of each step, constrained by the floor plan. If a trajectory converges into a single location, a backward propagation process labels the Wi-Fi acquisitions to the inferred locations.

C. LITERATURE COMPARISON

Different approaches try to automatise the fingerprints construction process leveraging crowdsourcing. However,

as limitations can be pointed out, a sufficiently scalable solution is still needed. Most solutions demand annotated landmarks as inputs or take advantage of a limited group of information sources, which independently present cumulative errors due to low-accuracy sensors and non-linear signal distribution. Furthermore, most solutions only focus on mapping Wi-Fi fingerprints to be deployed on smartphones. With increasing throttling and restrictions on Wi-Fi scans from Android and iOS, such solutions may stop working in real contexts.

To address these limitations, the proposed solution maps fingerprints of different sources depending on the use case and with the available data collected by crowdsourcing volunteers. The full process is done automatically without explicit manual effort from users during the collection campaign as, contrarily to most available solutions, there is no need to previously define any landmarks or to install additional equipment. Also, in a real deployment setting, users are not constrained by the crowdsourcing device usage and do not have to input any information or manual annotation, as the full process is done unsupervisedly. These reasons may have a positive impact on users' adherence to the data collection. Although our approach is based on particle filtering as some previous works, it improves the traditional inertial sensing-based mapping process with more layers of information, as the geomagnetic field and the Wi-Fi network if available. Leveraging these sources, we can identify similarities between acquisitions, discovering which were collected in the same locations and therefore should be mapped together. This innovative process eliminates any ambiguity regarding the possible fitting of each trajectory within the maps, common in traditional approaches, and which escalates in buildings with similar floor plans in different storeys. In this sense, the proposed solution also addresses multi-storey buildings, while most literature solutions only consider one floor without the possibility of transitions.

The innovative aspects proposed in our solution ensure the accurate fingerprints construction, which is verified in the experiments we conducted in two different venues.

III. MULTI-LAYER CROWDSOURCED FINGERPRINTS CONSTRUCTION

This work addresses current literature limitations with an innovative approach that leverages multiple sources depending on their availability from crowdsourced data, to autonomously construct environmental fingerprints for fingerprinting-based IPS.

Figure 1 presents an overview of the proposed multi-layer fingerprints construction process, which can be divided into five different modules. After the crowdsourced collection period, the first module deals with the processing of inertial data to understand users' motion while they move throughout the indoor environments. When Wi-Fi information is available from smartphones, a second module resorts to ML techniques to cluster such data, dividing buildings into smaller areas with similar radio patterns. An important step for the
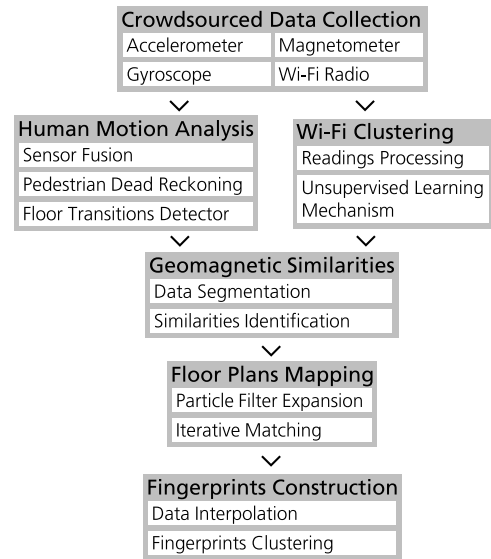

FIGURE 1. System overview.

accurate mapping is applied in the algorithm's third module, where geomagnetic data from different contributions is compared, to identify which were collected in the same locations. From that, the fourth module applies an iterative method to accurately map the estimated trajectories into the correct location of the floor plan, and into the correct floor on multi-storey buildings. After processing all crowd contributions, with all floor plans populated, fingerprints are constructed in the fifth and final module of this solution.

A. HUMAN MOTION ANALYSIS

The first module of the fingerprints construction process deals with the processing of inertial data, collected without any explicit effort from crowdsourcing users. IMUs embedded in most smartphones contain increasingly accurate accelerometers, gyroscopes and magnetometers. From such devices, we leverage pervasively collected linear acceleration, angular velocity and local geomagnetic field data, that is processed to analyse the crowd behaviour and understand their trajectories across the building. Different stages contribute to the movement inference of this module.

Magnetometers aim to locally register the Earth's magnetic field. Although smartphones apply a calibration mechanism to eliminate the soft and hard iron distortions, this process often fails to remove brief distortions caused by ferromagnetic materials, which enables us to leverage them in our algorithm (Section III-C). As sometimes sensors get severely uncalibrated, an initial process removes unreliable acquisitions, from the accuracy status provided by Android smartphones.

1) SENSOR FUSION

To crowdsource data from smartphones, it is essential to widen the devices' usage scenarios, independently of how users place them. Sensor fusion algorithms translate the

inertial and magnetic data from the reference frame of the device to the reference frame of the Earth, which is important for three reasons. Firstly, it allows the decomposition of geomagnetic field data into East, North and Up directions, allowing the generation of geomagnetic fingerprints for each axis. Secondly, it assists in obtaining the heading of the user at each step. Finally, it allows the application of more robust step detection algorithms. To achieve this translation, acceleration, rotation and magnetic data are combined through sensor fusion employing a complementary filter.

A complementary filter tracks the rotation of the user with the gyroscope while using the magnetometer and accelerometer as absolute references for stabilisation of North and Up directions, respectively. This is achieved by combining the high-frequency component of the gyroscope with the low-frequency components of the magnetometer and the accelerometer. The contribution of each of these components is determined by the parameter α according to the following Equation:

$$\alpha = \frac{\tau}{\tau + dt} \tag{1}$$

where τ is the time constant for the split between relative (gyroscope) and absolute (accelerometer and magnetometer) references and dt the sample interval. A value of $\tau = 0.5s$ was chosen, equal to the inverse of the typical walking frequency upper bound of 2 Hz [24].

2) PEDESTRIAN DEAD RECKONING

The movement of pedestrians is characterised using PDR techniques, where the motion of the user is evaluated at each step. This can be split into three distinct problems: step detection, step length and heading variation estimation.

TABLE 1. Architecture of the Deep Convolutional Network for step detection.

Layer	Channels	Filter Size	Activation	Shape
Convolution	2	64	ReLU	[66, 2]
Convolution	4	32	ReLU	[35, 4]
Convolution	8	16	ReLU	[20, 8]
Convolution	16	8	ReLU	[13, 16]
Convolution	16	4	ReLU	[10, 16]
Convolution	1	10	None	[1, 1]
Flatten	-	-	-	[1]

Step detection is achieved through the use of a Deep Convolutional Neural Network whose architecture is presented in Table 1. The network takes as input a sliding window of 1.28 seconds of acceleration data transposed to the reference frame of the user using the method proposed in [25]. The output is a time series bounded by the interval [0, 1] and can be interpreted as the probability of there being a step at each instant. This time series is filtered using a fifth-order low-pass filter with a cut-off frequency of 2 Hz. Steps are detected in this signal by identifying peaks with values above 0.1.

The Neural Network is trained using as ground truth the result of the step detection algorithm described in [5], which

is developed for a specific device placement, namely held in the hand as if the user was looking at the screen. Following the sensor fusion processing, together with the transposition of the reference frame of the device to the user's, described in [25], all contributions are aligned into the same reference, regardless of the device usage. As such, we can use the inertial data in a reference frame independent from the placement of the device, to train a Neural Network and create a step detection algorithm independent of this placement. Moreover, the adjustment of the aforementioned threshold allows obtaining an ideal threshold between sensitivity and specificity. Further developments on this algorithm will be addressed in future work.

The length of each step is computed using the method proposed by Weinberg [26]:

$$d = K\sqrt[4]{A_{max} - A_{min}} \tag{2}$$

where A_{max} and A_{min} are the maximum and minimum values of the vertical acceleration in the Earth reference frame for that step and K is a calibration constant, here set to 0.45.

Finally, the heading variation at each step is computed through the numerical integration of the z component of the gyroscope in the reference frame of the Earth. With all movement parameters obtained, it is possible to estimate consecutive positions between steps.

Although PDR can be affected by problems due to noise accumulation on inertial sensors, often causing drift on the heading or erroneous displacement estimation, our multi-layer solution mitigates these errors.

3) FLOOR TRANSITIONS

The path estimation is done across a two-dimensional plane, where the vertical movement of users is ignored by the employed methods. Therefore, considering the demand for a solution that works in multi-storey buildings, a floor transition detection mechanism was developed.

To efficiently detect when crowdsourcing users change floor, without any specific user annotation, we leverage the pressure data collected by devices' barometer. The atmospheric pressure is essentially stable at the same altitude, varying at different heights. However, in practice, unstable atmospheric conditions and factors such as the indoor humidity and temperature may affect the local pressure reading. Also, different sensors between devices may produce inconsistent readings. These reasons hinder the usage of the absolute pressure values to identify the floors where users are. Still, between devices, when the altitude of the sensing device changes, either in the upward or downward direction, the pressure reading changes accordingly, being lower in higher altitudes.

Therefore, we propose a threshold mechanism that processes the relative variations in barometric data for the detection of floor transitions. As the atmospheric pressure is affected by the momentary conditions of the venue, as its room temperature, initial filtering is applied to the collected signal, to remove the expected noise. Then, the smoothed

signal is normalised by its mean and standard deviation, followed by a peak detection mechanism of values above 0.1. The relative differences of the smoothed pressure value between those peaks are computed, and if any surpass the lower threshold of 0.25 hPa, the floor of the user changed. This threshold was defined from experiments in the university venue and may need to be adjusted when deploying our solution in other venues with different floor heights. Also, by the evaluation of the transition duration, it is possible to infer with high confidence the type of transition.

With this mechanism, in the university setting, we are able to detect when a user transitions one floor, its direction and type (stairs, lifts or ramps). In our study, the trajectories performed by participants only had at most one floor transition, so our algorithm only considers this scenario. However, as transitions of more than one floor will result in proportional multiples of pressure differences, we believe that our algorithm can be adapted for such scenarios, to be addressed in future work. Moreover, with drastic changes in the indoor atmospheric conditions, high variations in the local pressure readings may mislead to erroneous detection of floor transitions. The current mechanism does not deal with this problem, as during experiments it was not verified, but future developments will take it into consideration. Nevertheless, as our solution relies on crowdsourcing with multiple layers and a particle filter to expand particles into the floor plan, erroneous trajectories will likely not be mapped. If eventually they are, constructed fingerprints will not be affected given the large volume of data leveraged throughout this process.

4) DOMAIN CONVERSION

The final step of the motion analysis addresses the high variability of walking patterns between humans. People of different ages or in distinct contexts display different walking speeds, which greatly impacts signals acquisition. Considering the importance of having comparable magnetic and Wi-Fi signals in the next modules of our solution, we apply a domain conversion mechanism. The collected signals, originally in the time domain and referenced to a timestamp, are converted to the distance domain, with sensor readings indexed to a specific distance travelled by the user. Knowing both the timestamps of each sample and the walking parameters obtained with PDR, we apply a linear interpolation to estimate values between displacements.

For the collected geomagnetic field data, as sensors collect with high sampling rates, a fixed interpolation value can be chosen with negligible risk of deviated estimations. Considering both the needs for the accurate representation of the original signal and computational efficiency requirements, we selected an interpolation value of 10 cm.

On the other hand, Wi-Fi measurements consist of packages of information, received after requests from smartphones, which have a low sampling rate. For this reason, the domain conversion of Wi-Fi is done by estimating the displacement corresponding to the timestamp of each package, considering the steps before and after the reply timestamp.

B. WI-FI CLUSTERING

The second module of the presented algorithm clusters Wi-Fi data into groups of similar information, only possible in close areas of some location. Depending on the Wi-Fi readings restrictions from collection devices, this mechanism processes reply packages following device requests for surrounding Access Points (APs), to divide a floor plan into smaller areas of similar radio patterns.

For this purpose, the specifications of Wi-Fi networks are leveraged. Ubiquitous in indoor environments, such networks are employed in several IPS [5], [7], [16] and consist of multiple APs distributed throughout buildings. Each AP may have defined several Wireless Local Area Networks (WLANs), each one characterised by a unique Basic Service Set Identifier (BSSID). This important feature is registered in the reply packages received by the devices, together with the Received Signal Strength Indicator (RSSI), which allow the association of an AP to a specific location.

The use of radio signals for positioning presents some challenges, ranging from signal attenuation due to buildings' construction materials, to signal fluctuations and noise related to the dynamic changes in the environment, such as the human body itself or the device heterogeneity [9], [27]. These challenges affect the accuracy of IPS based only on Wi-Fi signals. Nevertheless, Wi-Fi networks still provide important information that, if available, we use to divide the floor plans into smaller areas, aiming to lower the errors of following modules and to optimise the computational efficiency.

Contrarily to IPS solely based on Wi-Fi, the aforementioned challenges do not greatly impact our unsupervised fingerprints construction solution. In this scenario, Wi-Fi data is used in the clustering to divide buildings into smaller areas, to facilitate further modules. Still, before clustering Wi-Fi data, an initial pre-processing step is applied to reduce signal's noise due to interferences and devices' variability.

Although APs are fixed in the same location and work generally with the same transmitting power, the produced signal is highly variable due to interferences. As such, we apply a noise removal mechanism to increase trust in the clustering mechanism. Firstly, a search over all replies from previously crowdsourced acquisitions removes APs that never register RSSIs above -50 dBm neither have a variation between collected values higher than 30 dBm, as they have low discriminative power. An additional process eliminates all RSSIs below -80 dBm, as low values present ambiguous information since they can either be due to far distances from the AP or shorter distances with high attenuation from thick walls, for example. The WLANs operating in the 5 GHz radio band are also eliminated from the clustering mechanism, since older devices cannot detect them. Each reply package is an individual object to be clustered, containing as features the information of all APs ever detected in the building.

Regarding device heterogeneity between collection devices, which results in variations in the signal strength measured at the same time and place, each reply package is individually normalised by the maximum and minimum values. All previously removed or non-existing RSSIs assume the value of -1, contrarily to remaining RSSIs that take values in the interval $[0, 1]$. With this pre-processing step we address most issues that can jeopardise the use of Wi-Fi signals.

The applied clustering algorithm is described in detail in [12]. Due to factors such as the computational complexity given the high number of features, the K-Means algorithm was chosen. This unsupervised ML algorithm optimises clusters by assigning each object to its closest centroid. In an iterative process until reaching convergence, the centroids are recomputed and objects reassigned. K-Means is a partitional clustering algorithm, which requires setting K, the number of clusters. As we aim to build an unsupervised algorithm, such information is not available. Therefore, we employ the method of Zhang *et al.* [28], which uses the sum of the squared distances between each object and its centroid for the different number of clusters, to compute, from the obtained graph, the maximum curvature point. This value is the ideal number of clusters, therefore the selected K. Due to Wi-Fi throttling in some devices, sampling rates are decreasing to as low as four Wi-Fi scans in each two-minute period. Consequently, the outliers removal mechanism of [12] is dismissed, as it is not possible to ensure that between two consecutive replies, the user did not pass in a different cluster area.

The automatic clusters selection process enables the application of this method in different scenarios, since the number of identified Wi-Fi patterns will increase with the size of the building. Although the maximum K value is set at 10 due to the algorithm limitations when testing in more clusters, this value is reasonable for most scenarios. If in future work we face cases where 10 clusters are insufficient, new methods for the automatic selection will be researched. Also, with the expansion of the crowdsourcing datasets in such scenarios, the clustering algorithm may take more resources to reach a convergence point. Nevertheless, as our solution will run offline after an initial collection campaign, no major problems are expected to come with the increased complexity.

C. GEOMAGNETIC SIMILARITIES

Before applying a particle filter to fit crowdsourced acquisitions to a building's floor plans, the third module of our algorithm ensures the process is done with high accuracy. The Earth's magnetic field is thus used in this context to identify which acquisitions were collected in the same location.

Although the geomagnetic field is essentially stable around the same region, it is highly affected by construction materials and electrical equipment. These cause specific and persistent interferences on the field, that produce unique patterns on the collected signals. With this useful information, we can identify precise locations within the crowdsourced data. As such, we apply a comparison mechanism to identify similarities between acquisitions.

1) TRAJECTORIES SEGMENTATION

The amount of data generated with crowdsourcing poses a problem to extensively compare individual signals to each other. The quadratic complexity of the problem requests the limitation of the comparisons set. Considering this, we apply a segmentation mechanism to the inferred trajectories, so it is possible to only retrieve signals that provide the most useful information for the similarities identification process.

From the Wi-Fi clustering results, if available, an initial segmentation splits trajectories into sections that have consecutive Wi-Fi reply packages with the same cluster label. This is done to ensure that each new section fully belongs to the same area of the building.

A second segmentation step evaluates the shape of each section. The process to infer trajectories from inertial data is sometimes sensible to device movements that do not relate to the users' motion. Although sensor fusion aligns the devices to the Earth's reference, sudden and brief tilts on the phone may not be recognised and produce mistaken turns. As such, further segmentation extracts from the initial segments the straight portions, which do not suffer from this problem.

Based on the premise that longer similar magnetic sequences are more reliable regarding their uniqueness, a minimum threshold for the segment size is defined. This value results of a balance between the approximate length of the corridors of a building and the process efficiency. In both use cases we present, an office and a university, for generalisation, a minimum length of 5 meters was set. Still, the threshold for the university venue, as it is larger, could be more restrictive.

2) NOTABLE INSTANTS DETECTION AND SIMILARITIES IDENTIFICATION

When a segment does not vary much within itself, no interferences produced the unique patterns we aim to find, so it has insufficient information to produce a robust comparison. As such, to ease the process of comparisons between previously segmented sections, geomagnetic similarities are only computed using segmented magnetic field signals that present a magnitude standard deviation higher than a threshold, defined to be 1 μT in both use cases.

After this selection process, the most notable instant of each segment is calculated using a self-similarity cost matrix that comprises the multidimensional Euclidean distance between each instant of the segment and its remaining instants. The multidimensional distance includes the intensity value and the first derivative of the three axes of the magnetic signal resulting in a 6-dimensional vector. The first derivative is used to capture the shape of the signal, since different smartphones have usually different offsets in the magnetic field readings. Inspecting the self-similarity cost matrix, the most notable instant is the one that produces the maximum cost compared to the rest of the segment. This process is exemplified in Figure 2, where the self-similarity cost matrix from a 1-axis signal is drawn, together with resulting summed
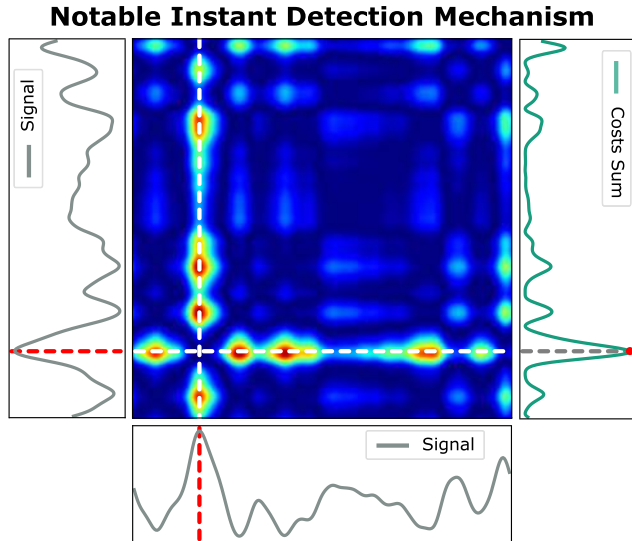
Notable Instant Detection Mechanism

FIGURE 2. Process of the most notable instant detection, for a 1-axis signal, which corresponds to the instant of the maximum sum of costs, obtained from the self-similarity cost matrix.

Segments Alignment

FIGURE 3. Alignment of two magnetic sequences from the similarities detection process between two contributions.

costs (in green), from which the identified maximum represents the signal's most notable instant (in red).

Next, the identification of segments that were collected in the same location is achieved by comparing pairs of signals from straight segments that present the same Wi-Fi cluster. Furthermore, with the absolute orientation known after sensor fusion, the process will also only match segments with concordant directions, with a maximum difference of 45°.

Since the obtained segments have different lengths, depending on the performed trajectories, the comparison between segments is done with the combination of two modifications of the Dynamic Time Warping (DTW) algorithm: the subsequence DTW [29] and the derivative DTW [30]. From a first signal, the subsequence to be searched among the segments that fit the previous conditions is retrieved from a pre-defined window size around its identified notable instant. In an iterative process, where the window size of the subsequence is progressively increased, the modified DTW algorithm is applied to obtain the warping path distances. Depending on both the resulting alignment and the computed distance value, the overlap of a subsequence to other segment is accepted or rejected, and the optimal window size is selected. Figure 3 depicts the resulting alignment from the comparison process between two magnetic sequences from different contributions, collected in the same location.

D. AUTONOMOUS FLOOR PLANS MAPPING
The innovative fourth module of the presented solution deals with the accurate mapping of crowd contributions into the correct locations, from the outputs of previous modules, which will be used to obtain environmental fingerprints. This fully unsupervised process only takes as inputs the floor plans of buildings, with only the annotation of floor transitions, as stairwells or lifts.
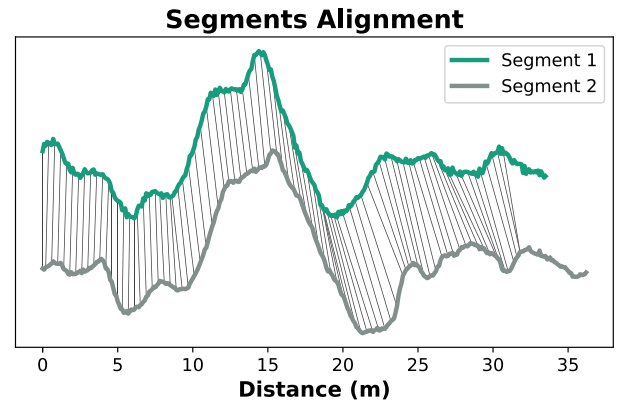
To achieve this, this module is divided into two different components, which recursively interact together until achieving an optimal convergence point. One of such components consists of a particle filter, which maps crowd contributions into possible locations of available floor plans, from the initial trajectories reconstruction information. Considering that multi-storey buildings often have overlapping characteristics between floors, a second component then ensures that routes are fitted into the correct location of the correct floor.

1) TRAJECTORIES MAPPING WITH PARTICLE FILTERING
The identification of possible locations for each acquisition is achieved by constraining PDR data to a floor plan using a variation of a Condensation particle filter, where each particle constitutes a set of four variables: position x, position y, heading y and significance s [31].

At each step, a step length l' and a heading variation $d\theta'$ are sampled for each particle from Gaussian distributions L and $d\Theta$ as such:

$$L \sim \mathcal{N}(l, l \times \sigma_l^2) \tag{3}$$
$$d\Theta \sim \mathcal{N}(d\theta, \sigma_\theta^2) \tag{4}$$

where l is the length of the step as determined by Equation 2 and $d\theta$ the original difference between the heading of the current step and the heading of the previous step. These are applied to the position of the particle as such:

$$
\begin{aligned}
p_h^{i,t} &= p_h^{i,t-1} + d\theta' \\
p_x^{i,t} &= p_x^{i,t-1} + l' \cos(p_h^{i,t}) \\
p_y^{i,t} &= p_y^{i,t-1} + l' \sin(p_h^{i,t}) \\
p_s^{i,t} &= (p_s^{i,t-1} \times P(L = l') \times P(d\Theta = d\theta'))^{\frac{1}{3}} \tag{5}
\end{aligned}
$$

where $p^{i,t}$ is particle i at step t. If the position $(p_x^{i,t}, p_y^{i,t})$ is not a walkable position, the particle is removed.

To counteract sample redundancy, particles are penalised for occupying the same grid square as other particles. This is

achieved by applying the following Equation:

$$p_s^{i,t} = \frac{p_s^{i,t}}{C^{0.5\exp(-0.5\frac{N}{A})}} \qquad (6)$$

where C is the number of particles in the same grid square as $p^{i,t}$, A the total number of occupied grid squares and N the maximum number of particles.

Finally, the particles are resampled with replacement. The probability of each particle being sampled is proportional to its significance. Therefore, at each new step from the pedestrian, a new generation of particles is created from the previous generation, considering for each particle the estimated step length and heading change, obtained from Equations 3 and 4, together with the introduction of random noise from Equation 5.

When the full route is expanded after the last step is processed, the resulting particles are clustered using DBSCAN. In each cluster the particle closest to its centroid is selected and a path is created by recursively tracing back its expansion history. Each path is compared to the path obtained by PDR using the following Equation:

$$D = min_{\theta\in[0,\,360[} \frac{1}{T}\sum_{t=0}^{T}(x^{pf,t} - (\cos\theta x^{dr,t} + \sin\theta y^{dr,t}))^2$$
$$+ (y^{pf,t} - (\sin\theta x^{dr,t} + \cos\theta y^{dr,t}))^2 \qquad (7)$$

where x^{pf} and y^{pf} are the x and y positions of a path from the particle filter, x^{dr} and y^{dr} are the x and y from dead reckoning and T is the number of steps. The path from the cluster with the lowest D value is chosen as the path reconstruction.

To deal with multi-floor mappings, the initial distribution of particles across the floor plans accounts for the detected floor transitions from the first module. Based on the premise that the existence of a transition restricts the possible positions within the building where the user was in that specific moment, such trajectories are expanded from an initial distribution of particles around the specific transition locations, as shown in Figure 4a. For example, if the floor transition detector outputs that the user went up a stairwell, then the algorithm will place particles around the stairwell locations, from which is possible to go up, as well as on their corresponding ends. From there, the particle filter expands the trajectory backwards, for the portion before the transition, and forwards for the portion after. If multiple transitions had occurred in the same acquisition, then the previous expansion would be performed until the next transition moment. Here, a further mechanism verifies if the last position is close to the corresponding transition type, which means the expansion was successful and can be continued in the other end of the stairwell, for example.

Contrarily, when a contribution was fully collected within the same floor, as the system cannot restrict the possible locations to start the expansion, particles are distributed across the full area of the floor plans and expanded forward from the initial moment. In order to automatically scale the system to the size of the considered floor, instead of setting an initial
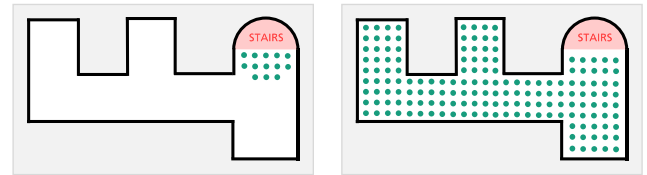
(a) Multi-floor initial particles distribution, from a detected transition by stairs.

(b) Single-floor initial particles distribution.

FIGURE 4. Difference between initial particles distribution from single-floor and multi-floor contributions.

number of particles, we distribute the necessary particles in a regular grid with a spacing of 0.6 m between them, as depicted in Figure 4b.

2) ITERATIVE ACCURATE TRAJECTORIES MATCHING
While the particle filtering component has a central role in mapping users trajectories into buildings floor plans, it alone cannot provide adequate accuracy to construct in an unsupervised way fingerprints for IPS.

As such, we deployed an iterative method that progressively maps users contributions to their correct locations, relying on the geomagnetic similarities identification from Section III-C.

Algorithm 1 describes the developed iterative method. During this process, depending on the particle filter expansion results, trajectories can be stored in three different categories. When the algorithm is certain that some acquisition is accurately mapped, it stores the trajectory as a final mapping in *mappedList*, and can be used to aid the mapping of others. If a trajectory could be fitted into one or more floor plans, the algorithm classifies the mapping as ambiguous, so it will be stored in *completeQueue*, as further validation is needed. At last, usually due to dead reckoning problems, the particle filter may fit trajectories incompletely on the floor plan. If they are long enough and got the major part mapped, *incompleteQueue* stores such trajectories to be verified later.

Firstly, based on the retrieved segments' length and the number of detected floors, trajectories are classified into three score levels of decreasing relevance (*cl* value in Algorithm 1). This process orders which acquisitions have more information for the initial mapping with the particle filter.

Starting with acquisitions with the lowest score level, i.e., when *cl* is equal to 1, the particle filter tries to map them into the available floor plans. The successful mappings are stored in *completeQueue*, to be then tested to verify if previously identified magnetic similarities exist among them and if the corresponding locations are close enough. In that case, such trajectories are considered to be mapped and those crowd contributions are accepted and stored in *mappedList*. When no overlaps are confirmed, acquisitions are maintained in *completeQueue* until a new verification is conducted in a subsequent iteration. Depending on the existence of successfully mapped routes in *mappedList*, the next step uses geomagnetic similarities to map new trajectories using Algorithm 2. After

this, or if *mappedList* remains empty, the classification score increases and the process is repeated until the maximum classification score is processed, i.e., when *cl* is equal to 3. After this moment, this method cannot accept as final any more complete mappings, so Algorithm 3 will verify if it is possible to use incomplete routes from *incompleteQueue* for the future fingerprints.

Algorithm 1 InitialFullMapping

Result: *mappedList*, *completeQueue*, *incompleteQueue*
for *cl = 1 to 3* **do**
    for *acquisition with classification == cl* **do**
        map trajectory with particle filter;
        if *mapping successful* **then**
            update *completeQueue*;
        end
        else if *mapping incomplete* **then**
            update *incompleteQueue*;
        end
    end
    verify existence of similarities between *completeQueue* mappings;
    if *similarities confirmed* **then**
        update *mappedList*;
        run MapFromSimilarities;
    end
end
run MapIncompleteTrajectories;

With a previous set of acquisitions successfully mapped in *mappedList*, Algorithm 2 maps new trajectories, from the existing geomagnetic similarities between them and the ones already mapped. Firstly, all similarities in *similaritiesList* are ordered by the optimal window size from the extension process and the lower distance value, obtained from the modified DTW described in Section III-C. Then, iteratively all similarities from *similaritiesList* are verified and when one is found between an already mapped and a new trajectory, the overlapping section is taken as the start, and from there the particle filter maps the remaining positions of the new acquisition. Since the algorithm is certain about the location of the already mapped acquisition, we can take the outputs of the particle filter as the accurate mapping of the new, to be stored in *mappedList*. If the particle filter outputs an incomplete mapping that meets the minimum requirements, the trajectory is added to *incompleteQueue*. Finished the process, a new search verifies if, among the mapping in *completeQueue*, it is possible to verify from the overlaps, the mapping of any acquisition with the ones recently mapped.

When Algorithms 1 and 2 reach a convergence point where no more trajectories can be added to *mappedList*, a further search in Algorithm 3 verifies if it is possible to add stored incomplete routes from *incompleteQueue* to the final mappings, from the remaining similarities. If some incomplete mappings are accepted, they are transferred to

---

Algorithm 2 MapFromSimilarities

Result: *mappedList*, *completeQueue*, *incompleteQueue*
sort *similaritiesList*;
while *similaritiesList not empty* **do**
    nMappings = len(*mappedList*);
    for *similarity in similaritiesList* **do**
        if *both acquisitions mapped* **then**
            erase similarity;
        end
        else if *one acquisition mapped* **then**
            map new trajectory with particle filter from overlap;
            if *mapping successful* **then**
                update *mappedList*;
                erase similarity;
                break;
            end
            else if *mapping incomplete* **then**
                update *incompleteQueue*;
            end
        end
    end
    verify existence of similarities with *completeQueue* mappings;
    if *similarities confirmed* **then**
        update *mappedList*;
    end
    if *len(mappedList) == nMappings* **then**
        break;
    end
end

---

mappedList and Algorithm 2 will verify if it is possible to expand unmapped trajectories from the overlaps with the new additions. This process is repeated until reaching a new convergence point, where no more incomplete mappings can be accepted with certainty.

Algorithm 3 MapIncompleteTrajectories

Result: *mappedList*, *completeQueue*, *incompleteQueue*
while *incompleteQueue not empty* **do**
    verify existence of similarities with *incompleteQueue* mappings;
    if *similarities confirmed* **then**
        update *mappedList*;
        run MapFromSimilarities;
    else
        break;
    end
end

After convergence of all processes, no more acquisitions can contribute to the crowdsourced buildings' fingerprints. Although some remaining trajectories in the queues may be correct, its accuracy cannot be assured by the solution. With this, the cost of discarding some users' contributions is

assumed, to ensure that all accepted mappings are done with high confidence, from which the necessary fingerprints may be constructed.

E. FINGERPRINTS CONSTRUCTION

With the results from the trajectories mapping process, each crowd contribution now has the information of its real location on the building. From the set of acquisitions collected on each floor, the last module of our solution is able to autonomously produce the environmental fingerprints for fingerprinting-based IPS. Although in our use case, the geomagnetic field and the Wi-Fi are the leveraged sources, the process is extensible to more sources of information.

The fingerprints construction process is essentially similar for both sources. Fingerprints consist of maps resembling the floor plans of a building, with the annotation of the expected readable value of each source at each position. These maps have a predefined resolution, which is chosen depending on the desired localisation resolution and the source sampling rate.

The process takes an empty map of all walkable locations of the building, one for each magnetometer axis and one for each Wi-Fi BSSID. Then, each map position will get the reading values of all previously mapped acquisitions that pass by. As magnetometers collect with high sampling rates, it is possible to retrieve a reading from almost any resolution. In the case of Wi-Fi signal, the empty maps receive the readings from the mapped positions that correspond to all received packages. After this annotation process, each fingerprint position may have several values from different contributions. Considering that some acquisitions may be influenced by anomalous fluctuations, each fingerprint position assumes the median value from all that were registered.

As a result of this process, some positions may not be mapped as no accepted acquisitions passed by. We then apply a further interpolation to minimise this problem using a Gaussian kernel around each unmapped position with a predefined interpolation window. The interpolation process iterates over all possible positions of the fingerprint that do not possess a previously mapped value. Then, the value for the current unmapped position is the average of the mapped positions within the kernel weighted by their distance to the unmapped positions using the Gaussian kernel. If there is only one mapped value, then, the new value will be equal. If there are no previously mapped values within the kernel, the position will remain unmapped. This process is repeated for all unmapped positions. In the end, a smoothing algorithm is applied. It iterates over all fingerprints positions, and using the previous kernel dimensions, the mean of all values within the range is calculated, which will be assumed as the new value.

The large range of available Wi-Fi equipment works under international standards, but manufacturers can change some devices' settings, which affect networks configurations. As an AP may have different BSSIDs, even working on the same radio band, the size of such data, especially in large

buildings, may be impracticable in terms of computational costs. As it is not possible to unambiguously define which BSSIDs belong to the same AP, we apply an unsupervised ML process to cluster all Wi-Fi fingerprints into a smaller set that contains all information.

To cluster the obtained fingerprints, we begin by defining a suitable distance metric. First, the RSSI values are rescaled to be bound by the interval [0, 1]. Assuming a minimum value of -100 dB and a maximum value of 0 dB, this is achieved by applying the following Equation:

$$RSSI_{x,y}^{r,i} = (RSSI_{x,y}^i + 100)/100 \qquad (8)$$

where $RSSI_{x,y}^i$ is the RSSI value of fingerprint i at the position x, y and $RSSI_{x,y}^{r,i}$ the re-scaled value. The distance metric is then defined as such:

$$d^{i,j} = \frac{\sum \|RSSI_{x,y}^{r,i} - RSSI_{x,y}^{r,j}\| \times (RSSI_{x,y}^{r,i} + RSSI_{x,y}^{r,j})}{\sum (RSSI_{x,y}^{r,i} + RSSI_{x,y}^{r,j})} \qquad (9)$$

The resulting distance matrix is then used with DBSCAN to cluster the fingerprints, and outliers are removed. Finally, the fingerprints of each cluster are combined by taking the median value at each coordinate.

The presented solution outputs environmental fingerprints that follow the provided floor plans' of buildings. In our use case, fingerprints for all geomagnetic field axes and clustered fingerprints for the detected Wi-Fi APs are produced. The first are collected with a resolution of 20 centimetres, while the second have a resolution of 1 meter, given the lower sampling of Wi-Fi measurements.

IV. SYSTEM EVALUATION

This Section deals with the validation of the proposed method, to assert its applicability in any indoor scenario. For this purpose, two validation strategies were implemented. Firstly, the crowdsourcing fingerprints obtained with our solution were compared to those obtained from traditional methods. The point-by-point differences provide an insight of how similar both types are, and if changes in localisation are to be expected when replacing the manual fingerprints. Next, in order to deeply understand the impact of the crowdsourcing fingerprints in a real setting, we used a set of test acquisitions as the input for a fingerprinting-based IPS [5]. By evaluating the localisation performance attained by the same data but using the different types of fingerprints, we can verify the potential of crowdsourcing for this purpose. At last, we asserted the computational complexity of the presented solution, with tests regarding the time and memory requirements considering different use cases.

We tested our solution in two different settings, a single-floor smaller office building and a larger multi-floor university. These two distinct environments aim to verify the achieved results in different deployment use cases. In both settings, with a crowdsourcing-based approach, groups of users with different Android smartphones collected data while walking throughout the buildings. A logger app was
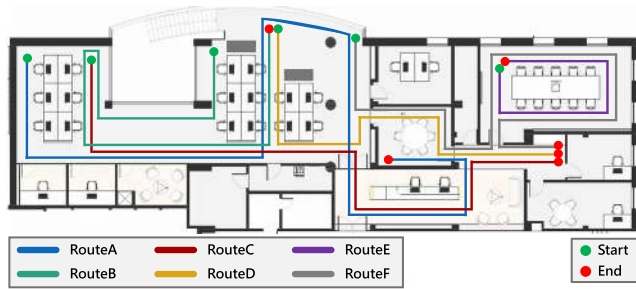
FIGURE 5. Example set of six routes designed for the office building. Crowdsourcing users were instructed to start the trajectories at the green circle and finish at the red circle.

provided to register the available data. A set of routes was predefined in both venues, to provide ground truth information for the evaluation. Figure 5 schematises six of such routes on the office building, from the total of 51 routes designed for both venues. The test routes cover the entire buildings area, considering that some locations should be crossed in different directions and different times of the day, to ensure data variability. The crowdsourcing volunteers were then instructed to start at the green circle and finish at the red circle. Also, the moments of each change of direction were annotated on the logger app, to provide ground truth information for the localisation results evaluation. In each venue, the data of one user was excluded from the proposed fingerprints construction process, so validation tests do not produce biased results against repeated movement patterns or behaviours.

The first setting is an office building with a single-floor and an accessible area of 205 m^2 (Figure 6a). In this dataset, six users collected data over 22 predefined trajectories, totalling 135 acquisitions for 95 minutes. From this set, 22 (16.3%) contributions from a user were left out for further validation. Two smartphones were used for the acquisitions (LG Nexus 5 and Huawei Nexus 6P), being handled in texting position. From the geomagnetic similarities identification process, 68 of total contributions (60.2%) had overlaps identified. From all similarities, 79.6% were effectively collected in the same sections of the building. From those possible to be mapped acquisitions, 66 (97.1%) were fitted into the floor plan and contributed to the fingerprints. This represents 58.4% of the total usable dataset. All routes were mapped into the correct locations, although 15 had minor fails, as in the case of expanding to a near parallel corridor. Nevertheless, this reduced number of errors is not expected to greatly affect the results of the crowdsourced fingerprints.

The second venue is a university with two interconnected buildings, from which we collected data over three different floors, with transitions of different types (Figure 6b). This setting extends the results from the previous venue as it resembles more common use cases with the inclusion of some open spaces. For a total area of 3900 m^2, six users collected 167 acquisitions with seven smartphones (LG Nexus 5 and G7, Google Pixel and Pixel 3, Samsung S9, Huawei Nexus 6P and Xiaomi Mi8), placed either on the
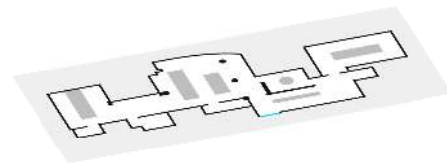
(a) Office building floor plan.
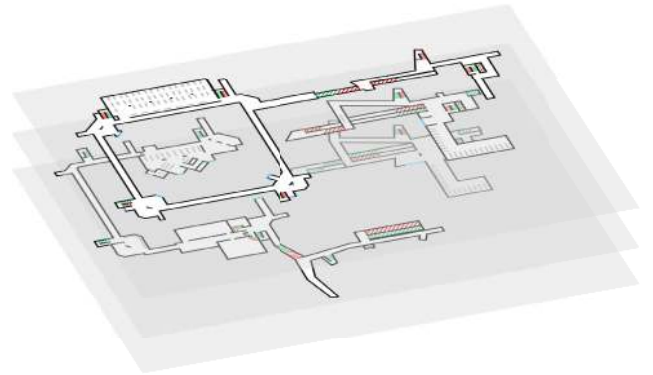
(b) University buildings floor plans.

FIGURE 6. Buildings floor plans.

hand in texting position, or in the pocket. 52 acquisitions were excluded by the uncalibration detection process. From the remaining set of 115 contributions, totalling 351 minutes, 17 of such acquisitions (14.8%) were not used, for further validation. As this building contains larger open space areas, to ensure covering the full space, the 29 designed routes included free movement areas. Resulting from our solution, in this venue 66 acquisitions entered the mapping process (67.3%), as they had identified similarities. 54.2% of all similarities were collected in overlapping locations, a lower value justified by the standard similarity threshold. 48 (65.8%) of usable acquisitions were mapped, totalling 49.0% of processed contributions. From the mapped set, three routes were mapped in the wrong floor and minor mistakes were identified only in six acquisitions, with the major part in the correct locations. Again, this is often due to erroneous expansion to parallel areas, caused by undetected steps or inaccurate stride length estimation.

From the presented numbers, the number of crowd contributions that were effectively used to construct the required environmental fingerprints may seem quite low. However, with users freely moving with the smartphone in not completely fixed positions, the acquisitions may be affected by some errors, which in the end diminishes the confidence that the system has in such contributions, being discarded throughout the process. This ensures that the produced fingerprints present a competitive accuracy for a system like ours to be deployed in any indoor setting.

A. FINGERPRINTS COMPARISON

To compare the results between crowdsourced fingerprints and traditional ones, we computed the absolute differences point by point, for all magnetic axes and Wi-Fi APs.
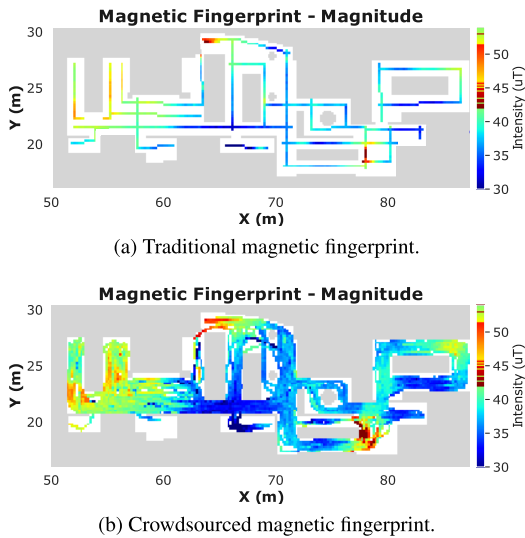
(a) Traditional magnetic fingerprint.

(b) Crowdsourced magnetic fingerprint.

FIGURE 7. Constructed magnetic fingerprints before any interpolation, obtained by the traditional and crowdsourcing methods, respectively. Both fingerprints show the magnitude of the three axes of the magnetic field.

(a) Traditional magnetic fingerprint.

(b) Crowdsourced magnetic fingerprint.

FIGURE 8. Interpolated magnetic fingerprints for the magnitude of the three axes, collected, respectively, by the traditional and crowdsourcing methods.

TABLE 2. Statistical metrics of values differences between traditional and crowdsourced fingerprints.

	Magnetic Field (μT)		Wi-Fi (dBm)	
	Office	University	Office	University
Mean	3.0	6.0	3.2	4.9
Standard Dev.	2.0	6.5	3.0	4.7
Median	2.4	3.9	2.0	4.0
Percentile 75	3.9	8.0	5.0	7.0
Percentile 90	5.8	13.5	7.0	11.0

Traditional fingerprints were collected by the method described in [5], on which a user manually collects data throughout the buildings with a smartphone. Although this method provides ground truth coordinates for fingerprints construction, due to its time-consuming procedure, the data collection process is performed by a single device in a predefined time of the day. On the other hand, crowdsourced fingerprints include contributions from multiple users over different moments and using different devices. However, they lack ground truth coordinates, which can contribute to erroneous mappings.

Therefore, in this comparison, we are only interested in evaluating the differences between both methods of fingerprints construction. Since crowdsourced fingerprints rely on human motion analysis, contrary to traditional fingerprints that use ground truth coordinates, the distribution of sensed values will not necessarily be concordant. This increases the difficulty of the comparison process. For this reason, before computing the absolute differences point by point, unmapped areas in the fingerprints are interpolated using the methods described in Section III-E.

To schematise this process, Figure 7 shows the constructed geomagnetic fingerprints of the magnitude of all axes from both processes, before any interpolation. While Figure 7a has the data collected throughout the ground truth positions, which the expert provided to the system, Figure 7b has the crowdsourcing fingerprint, automatically constructed by our solution. In the last, each position, represented by each small square, contains the median between all contributions mapped into it.

On the other side, Figure 8 shows the same fingerprints after the interpolation process. While Figure 8a contains the interpolation output corresponding to the traditional finger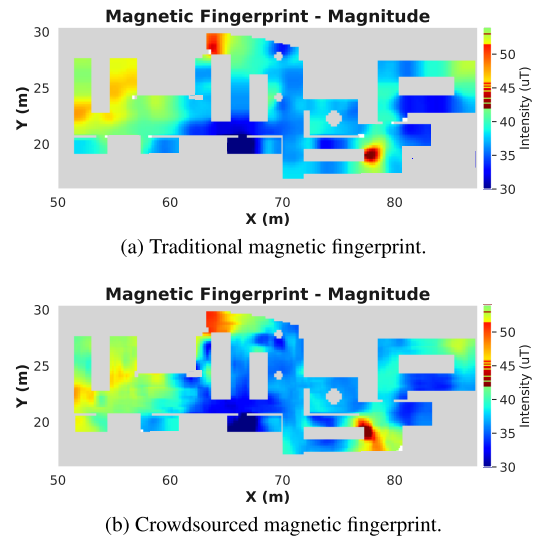print, Figure 8b includes the interpolation result from the crowdsourcing method. After the interpolation process, we can provide a more complete point-by-point comparison between both types of fingerprints. Furthermore, these results allow for a visual comparison between both methods. Although some differences can be denoted, the general colour pattern is very similar, as most contributions were mapped into the correct locations.

The results of the fingerprints comparison process are available in Table 2. These metrics were computed from the point-by-point absolute differences between the three-axes magnitude values in the case of geomagnetic field, and between the mean differences of all APs in the case of Wi-Fi. The presented performance metrics allow concluding that the signal differences between traditional and crowdsourced construction processes are relatively low, which supports the applicability of our solution in real settings. Nevertheless, the fingerprints differences are generally higher in the university venue than in the office. This is due to the data variability originated by the larger set of acquisition devices in the university, which creates higher differences when compared to the traditional fingerprints with a single device, even though the positioning results may actually be improved. Also, the amount of acquisitions that finished the mapping process and contributed to the fingerprint is comparably lower to the office building.
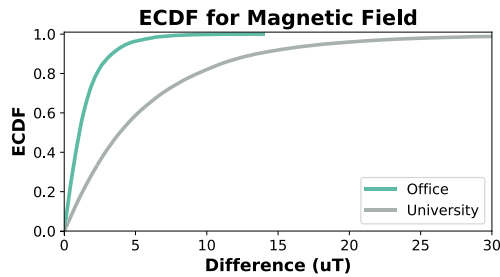
(a) Magnetic field fingerprints ECDFs.
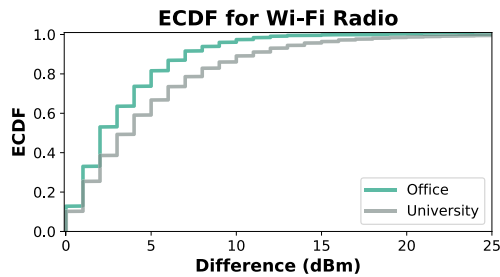
(b) Wi-Fi fingerprints ECDFs.

FIGURE 9. ECDFs resulting from the comparison processes between original and crowdsourced fingerprints, where the point-by-point signal differences were computed for the presented venues.

Figure 9 represents the Empirical Cumulative Distribution Functions (ECDF) that sum up the presented metrics. In Figure 9a, the ECDFs for the magnetic fingerprints comparison for all axes of the available floors are displayed, while Figure 9b presents the ECDFs for the Wi-Fi fingerprints comparison for all APs. The better results of the office building can be here denoted too.

B. LOCALISATION PERFORMANCE

Next, to understand the performance of crowdsourcing fingerprints in real scenarios, we relied on the fingerprinting-based IPS developed by Guimarães *et al.* [5], which tested the positioning results with the crowdsourced fingerprints against the traditional ones. This system relies on inertial, magnetic and Wi-Fi data, collected from smartphones, to locate users using a particle filter. By expanding the particles across the floor plan at each detected step, considering the match of sensor readings with the fingerprints, this solution is able to locate users in real-time. For the purpose of this evaluation experiment, we relied on the also available offline mode, which takes previously acquired data and applies the same techniques as in real-time. To allow the system evaluation, this IPS can check some positions of the designed trajectory, annotated by the user during the acquisition. These expected locations are compared with the positions achieved by the system, given by the centroid of all particles at each step. The closer each centroid is to the expected location, the higher is the system performance. As such, to evaluate the quality of crowdsourcing fingerprints, we submit a set of test acquisitions to this IPS, using each type of fingerprint, and

TABLE 3. Summary of characteristics of the test set for both the office and the university venues.

	Office	University
Total Test Routes	21	17
Average Routes Length (m)	38.5 ± 11.8	152.4 ± 57.2
Average Evaluation Positions	8.5 ± 2.2	7.0 ± 2.6

compare the difference between the expected and computed positions.

As the acquisitions of one contributor were left out from the construction process in each venue, we used their data in this evaluation, to ensure unbiased results. Table 3 summarises the main characteristics of the test sets for both venues, including the number of tested acquisitions, together with their average length and average number of evaluation positions. Although the trajectories made by the users are from the previously designed routes, it does not have influence in the results, as the continuous relation between consecutive sensed values is lost when constructing fingerprints. Each tested acquisition was run six times with both types of fingerprints, to accommodate the random factor in particles distribution.

We present the results through three metrics, namely the average error of the centroid throughout the ground truth evaluation positions, the final centroid error, and the final error of the particle with the highest probability. For each metric, the mean value of all runs from all tested acquisitions was computed.

For the office building, 22 different routes across the space were tested from one user, and Table 4 presents the comparative results. For the university venue, the contributor performed 17 acquisitions with different trajectories, and the localisation performance is available in Table 5. Each value in Tables 4 and 5 was obtained by performing the average error between all acquisitions, with the error of each acquisition achieved by averaging all six runs on the system.

In the first building, the initialisation of the IPS on each acquisition was achieved through the automatic distribution of particles, around the most similar area, from the Wi-Fi fingerprints comparison with the first received scan. Due to Wi-Fi acquisition constraints on the smartphones used in the second venue, which will be discussed below, here the initial position of each test was given to the system. Although different initial conditions are applied between buildings, the remaining localisation process runs similarly, which do not greatly affect the final results.

Regarding the office building, we verified that for the crowdsourcing fingerprints, constructed with the proposed method, the localisation performance actually exceeds the traditional method. This may be explained by the fact that the new fingerprints are constructed with more information, either due to the more data included, or the higher variability achieved by the different collection devices. These characteristics approximate the new fingerprints to reality.

On the other hand, the localisation performance of the university venue is lower, when compared to the office

TABLE 4. Localisation performance of the test set on the office building with the crowdsourcing fingerprints, compared to those collected by the traditional methods.

	Office Localisation Errors (m)	
	Crowdsourcing Fingerprints	Traditional Fingerprints
Average Centroid Error	3.35	3.94
Final Centroid Error	3.19	3.70
Best Particle Final Error	2.85	3.69

TABLE 5. Localisation performance of the test set on the university venue with the crowdsourcing fingerprints, compared to those collected by the traditional methods.

	University Localisation Errors (m)	
	Crowdsourcing Fingerprints	Traditional Fingerprints
Average Centroid Error	4.89	5.55
Final Centroid Error	6.17	6.21
Best Particle Final Error	7.31	7.46

building, even though the initial position of the user was given. These generally worse results are verified in both traditional and crowdsourcing fingerprints. Different reasons explain this difference and are related to the inner characteristics of the utilised IPS. Firstly, the system was until this moment never tested in such a large venue. The inherent sensor errors accumulate over time, and although correction mechanisms address some of them, problems such as missing steps or heading drift may still happen, which in a larger environment can affect the localisation process. Secondly, in this venue, we came across unusual Wi-Fi network settings. Fingerprinting-based IPS often rely on Wi-Fi maps, where one is obtained for each AP, with a specific signal decay pattern, continuously descending from the AP location. However, this venue's network works under a Single Channel Architecture (SCA), in which multiple APs operate in the same frequency channel and present to clients a single BSSID. Throughout the building, devices sense a stable signal strength, as a central controller decides which AP each device connects to. Although this setting provides a better user experience, it clearly causes problems in systems that expect to match Wi-Fi readings to specific areas of different fingerprints, so they can then be combined to contribute with a restrict possible location for the particle filter expansion. Together with this issue, most of the used smartphones run on Android versions that already constrain Wi-Fi scans to the limit of four requests in every two-minute period, which in the end provided fewer data to be used, the reason why we gave the initial position of each tested acquisition to the localisation system. This is a problem that, as addressed in Section II, will limit Wi-Fi-based IPS. However, as our solution proposes, the construction of multi-layer fingerprints helps in overcoming these issues. As the tested IPS relies on different sources of information, namely the inertial tracking, Wi-Fi and magnetic field [5], the system is still able to work and obtain a continuous location for the user, with an error in a range that fits most localisation scenarios.

Nevertheless, when evaluating the results of the crowdsourcing fingerprints by comparing relative differences between both methods, we conclude that the presented method achieves slightly better results, with performance errors generally lower than the ones achieved with traditional fingerprints. This proves that even though the university venue includes less mapped acquisitions than the office building, especially if we consider the area difference, 3900 m^2 to 205 m^2, respectively, the constructed fingerprints are well

suited for the deployment on a real localisation application. As such, with more available contributions from more users and devices, the method is expected to produce more accurate fingerprints, that may even exceed the results of the traditional construction methods, as verified in the office building.

We believe that the two presented scenarios provide a broad representation of the use cases that can benefit from this type of solution. Both the office and the university venues include several features that are present in most buildings, and account for their challenges, such as multiple floor transitions and open spaces. Nevertheless, more use cases could be tested to confirm the attained results, which will be considered in future work.

C. SYSTEM COMPLEXITY
To verify that our solution is deployable in most indoor localisation scenarios, we performed a study of the computational complexity of all modules. This estimation is not trivial, as the presented system contains several procedures that depend on a large number of variables and often in the outcomes of previous steps. Nevertheless, we can estimate which modules can escalate in larger venues and with more data.

Regarding the human motion analysis module of Section III-A, it has a complexity of $O(n)$, where n is the number of available acquisitions. Still, depending on the length of the acquisition, the processing time will also vary.

Next, the module of Section III-B, which performs the clustering of Wi-Fi data, presents a complexity of $O(r.s^{\frac{k+2}{p}})$, where s represents the number of Wi-Fi scans to be clustered, k the number of clusters and p the number of features. In our automatic selection of the number of clusters, we extend the computational complexity of the K-Means algorithm [32], with an iteration over r, the number of clusters to test. This variable should not exceed 10 clusters, which will not have a great impact on the complexity.

The third module of our solution, described in Section III-C, has a greater impact on the system complexity. While the trajectories segmentation process has linear complexity, $O(n)$, as it varies with the number of acquisitions, the notable instants detection algorithm is applied to each segment, having a complexity of $O(s)$, where s is the number of segments. In larger venues, where more and longer acquisitions can be potentially acquired, the number of segments will increase. This will have an impact on the similarities identification, which presents a worst case complexity of $O(l.s^2)$, with s the number of segments and l the length of the shorter

TABLE 6. Computational costs of the presented solution in the two presented venues, the office with one floor and the university with three floors, using 10 and 100 (98 in the university) acquisitions.

	Office		University	
	Time (s)	Mem. (Mb)	Time (s)	Mem. (Mb)
10 routes	155	260	1347	672
100 routes	840	522	147973	1113
Factor	5.4	2.0	109.9	1.7

segment between each pair to be compared, included due to the iterative process of increasing the window length. Our modification to the DTW itself presents a complexity of $O(w^2)$, with w representing the size of the window. As such, longer segments will have more windows tested, which are iteratively extended, thus impacting in the cost of the algorithm. These complexity limitations support the need for the reduction of the number of compared segments, either by the Wi-Fi clusters identification and the verification of segments' absolute orientation.

The mapping of trajectories into the floor plans, presented in Section III-D, can be divided in different processes. Firstly, in Algorithm 1, trajectories are mapped into the floor plans, having a complexity of $O(n.f)$, with n the number of acquisitions and f the number of floors. Next, the iterative accurate trajectories mapping from similarities, presented in Algorithm 2, has a complexity that tends to $O(o^2)$, with o the number of overlapping pairs of segments from the previous module. Algorithm 3 depends on the number of incomplete routes, i, presenting a complexity of $O(i)$.

Finally, the complexity of the fingerprints construction is $O(f.a)$, which linearly depends on the number of floors of the venue, f, together with their area, a.

To verify these complexity estimations, we present in Table 6 the computational costs regarding time and memory of our solution, for the two presented venues, with 10 and 100 acquisitions. We performed these tests in a laptop with an Intel Core i7-10750H processor with 12 cores at 2.60 GHz and 32 Gb of RAM memory.

From the results, it is clear that the university venue has a higher computational cost than the office building, both in terms of memory and time. This difference is visible even within the same dataset size. As explained, besides the number of acquisitions, the number of floors and the area of the buildings highly affect the cost. With longer acquisitions from contributors, more straight segments will be retrieved, which will be longer given the long corridors. Therefore, both the geomagnetic similarities and the floor plans mapping will take more time and memory to process.

Although the complexity of the presented solution is not ideal, it does not greatly affect its scalability to other scenarios, as the overall process will run on the cloud after a data collection period with crowdsourcing. Nevertheless, in the future, the complexity of these innovative algorithms can be improved before the deployment in real use cases.

Regarding the acquisition costs on the crowdsourcing contributors' devices, it is limited to the collection process. A logger app running ideally on the background will pervasively collect readings from the required sensors, with a sampling rate that can be optimised considering the device characteristics. Then, when the device is connected to a Wi-Fi network, the collected data will be sent to a server to be processed. An accurate estimation of the performance and battery costs on the smartphones will be conducted once our solution is to enter production.

V. CONCLUSION

This paper presents an innovative method for the automatic construction of environmental fingerprints for infrastructure-free fingerprinting-based IPS. We rely on crowdsourcing to collect large volumes of data, from a higher set of users and devices. Without any annotation from the contributors, we rely on the processing of multiple layers of information, to increase the confidence of the solution.

Through the integration of inertial tracking with the magnetic field and Wi-Fi data, we identify highly specific similarities that allow the identification of acquisitions collected in the same location. Taking advantage of buildings' floor plans, we apply a particle filtering approach, to expand each trajectory into the correct placement. A transitions detection mechanism detects when users change floors, so the mapping algorithm can use that information to construct fingerprints of multi-storey buildings. While our solution focuses on Wi-Fi and geomagnetic fingerprints, it can be easily adapted to produce maps for other environmental sources, such as Bluetooth.

While across the literature there are works in this topic, there is a lack of benchmark mechanisms to evenly compare solutions. Therefore, we evaluate our system on two different venues, by comparing at each position the values of the constructed fingerprints with the proposed method, to those obtained from the traditional manual collection process. Also, we verify the localisation performance using both types of fingerprints on the two presented buildings. With the obtained results, we ensure that our solution is able to provide effortless fingerprints mapping in real scenarios. As such, the deployment costs of fingerprinting-based IPS can be lowered, extending the usage scenarios of location-based services.

With the different sources of information leveraged in this work, we address the Wi-Fi scans limitation in smartphones. The restrictions applied tend to increase, which will limit the usability of current Wi-Fi-only solutions.

Regarding future work, the presented step detection mechanism and further stride length estimation process will be improved and validated with standard methods. Also, we will address the limitations of the current solution for the floor transitions detection, namely the susceptibility of the barometric data to unstable atmospheric conditions and the adjustment of the transition threshold in different venues and for multiple floor transitions. In this sense, an innovative algorithm based on deep learning for the floor transitions

detection is being developed, by using the discriminative power of Deep Convolutional Neural Networks to identify these transitions. In order to reach an even broader range of smartphones, this new module is being designed to work both with inertial and barometer data together, or inertial data alone. This module will infer the type of transition and its duration, allowing its segmentation and further use within the proposed system. This way, we believe that the technical challenges of using barometric data will be overcome.

Furthermore, as our work provides an automatic method for fingerprints construction when buildings change through time, the constructed maps may lose localisation accuracy. While in a real setting, a verification mechanism may trigger the automatic reconstruction of fingerprints, an update method to increasingly add informative data to the existing maps may be more optimal. As such, we leave this extension of our solution for future work.

At last, to reassure the achieved experimental results and to test the future developments, more use cases will be leveraged, and new trials will be conducted in different conditions.

REFERENCES

[1] *Solutions for Real-Time Location Systems (RTLS) by Infsoft.* Accessed: Feb. 15, 2021. [Online]. Available: https://www.infsoft.com/

[2] *Real-Time Location System (RTLS) for Indoor Tracking.* Accessed: Feb. 15, 2021. [Online]. Available: https://www.sewio.net/

[3] *Real-Time Location | RTLS | BLE Installation and Maintenance.* Accessed: Feb. 15, 2021. [Online]. Available: https://www.favendo.com/

[4] A. Alarifi, A. Al-Salman, M. Alsaleh, A. Alnafessah, S. Al-Hadhrami, M. Al-Ammar, and H. Al-Khalifa, "Ultra wideband indoor positioning technologies: Analysis and recent advances," *Sensors*, vol. 16, no. 5, p. 707, May 2016, doi: 10.3390/s16050707.

[5] V. Guimaraes, L. Castro, S. Carneiro, M. Monteiro, T. Rocha, M. Barandas, J. Machado, M. Vasconcelos, H. Gamboa, and D. Elias, "A motion tracking solution for indoor localization using smartphones," in *Proc. Int. Conf. Indoor Positioning Indoor Navigat. (IPIN)*, Oct. 2016, pp. 1–8, doi: 10.1109/IPIN.2016.7743680.

[6] F. Dwiyasa, M. Lim, Y. Ong, and B. Panigrahi, "Extreme learning machine for indoor location fingerprinting," *Multidim. Syst. Sign. Process.*, vol. 28, no. 3, pp. 867—883, 2017, doi: 10.1007/s11045-016-0409-0.

[7] G. Felix, M. Siller, and E. N. Alvarez, "A fingerprinting indoor localization algorithm based deep learning," in *Proc. 8th Int. Conf. Ubiquitous Future Netw. (ICUFN)*, Jul. 2016, pp. 1006–1011, doi: 10.1109/ICUFN.2016.7536949.

[8] G. Chatzimilioudis, A. Konstantinidis, C. Laoudias, and D. Zeinalipour-Yazti, "Crowdsourcing with smartphones," *IEEE Internet Comput.*, vol. 16, no. 5, pp. 36–44, Sep. 2012, doi: 10.1109/MIC.2012.70.

[9] G. Retscher, "Fundamental concepts and evolution of Wi-Fi user localization: An overview based on different case studies," *Sensors*, vol. 20, no. 18, p. 5121, Sep. 2020, doi: 10.3390/s20185121.

[10] X. Zhou, T. Chen, D. Guo, X. Teng, and B. Yuan, "From one to crowd: A survey on crowdsourcing-based wireless indoor localization," *Frontiers Comput. Sci.* vol.12, pp. 423—450, Jun. 2018, doi: 10.1007/s11704-017-6520-z.

[11] Y. Sun, Y. He, W. Meng, and X. Zhang, "Voronoi diagram and crowdsourcing-based radio map interpolation for GRNN fingerprinting localization using WLAN," *Sensors*, vol. 18, no. 10, p. 3579, Oct. 2018, doi: 10.3390/s18103579.

[12] R. Santos, M. Barandas, R. Leonardo, and H. Gamboa, "Fingerprints and floor plans construction for indoor localisation based on crowdsourcing," *Sensors*, vol. 19, no. 4, p. 919, Feb. 2019, doi: 10.3390/s19040919.

[13] W. Li, C. Zhang, Z. Liu, and Y. Tanaka, "Incentive mechanism design for crowdsourcing-based indoor localization," *IEEE Access*, vol. 6, pp. 54042–54051, Sep. 2018, doi: 10.1109/ACCESS.2018.2869202.

[14] G. Shen, Z. Chen, P. Zhang, T. Moscibroda, and Y. Zhang, "Walkie-markie: Indoor pathway mapping made easy," in *Proc. 10th USENIX Symp. Netw. Sys. Des. Imp. (NSDI)*, Lombard, IL, USA, 2013, p. 85—98.

[15] H. Luo, F. Zhao, M. Jiang, H. Ma, and Y. Zhang, "Constructing an indoor floor plan using crowdsourcing based on magnetic fingerprinting," *Sensors*, vol. 17, no. 11, p. 2678, Nov. 2017, doi: 10.3390/s17112678.

[16] B. Zhou, Q. Li, Q. Mao, and W. Tu, "A robust crowdsourcing-based indoor localization system," *Sensors*, vol. 17, no. 4, p. 864, Apr. 2017, doi: 10.3390/s17040864.

[17] W. Li, D. Wei, Q. Lai, X. Li, and H. Yuan, "Geomagnetism-aided indoor Wi-Fi radio-map construction via smartphone crowdsourcing," *Sensors*, vol. 18, no. 5, p. 1462, May 2018, doi: 10.3390/s18051462.

[18] C. Luo, H. Hong, and M. C. Chan, "PiLoc: A self-calibrating participatory indoor localization system," in *Proc. 13th Int. Symp. Inf. Process. Sensor Netw. IPSN*, Apr. 2014, pp. 143–153, doi: 10.1109/IPSN.2014.6846748.

[19] H. Shin, Y. Chon, and H. Cha, "Unsupervised construction of an indoor floor plan using a smartphone," *IEEE Trans. Syst., Man, Cybern. C, Appl. Rev.*, vol. 42, no. 6, pp. 889–898, Jun. 2012, doi: 10.1109/TSMCC.2011.2169403.

[20] J. Trogh, W. Joseph, L. Martens, and D. Plets, "An unsupervised learning technique to optimize radio maps for indoor localization," *Sensors*, vol. 19, no. 4, p. 752, Feb. 2019, doi: 10.3390/s19040752.

[21] J. Ahn and D. Han, "Crowd-assisted radio map construction for Wi-Fi positioning systems," in *Proc. Int. Conf. Indoor Positioning Indoor Navigat. (IPIN)*, Sep. 2017, pp. 1–8, doi: 10.1109/IPIN.2017.8115872.

[22] Z. Yang, C. Wu, and Y. Liu, "Locating in fingerprint space: Wireless indoor localization with little human intervention," in *Proc. 18th Annu. Int. Conf. Mobile Comput. Netw. Mobicom*, 2012, pp. 269–280, doi: 10.1145/2348543.2348578.

[23] A. Rai, K. K. Chintalapudi, V. N. Padmanabhan, and R. Sen, "Zee: Zero-effort crowdsourcing for indoor localization," in *Proc. 18th Annu. Int. Conf. Mobile Comput. Netw. - Mobicom*, 2012, pp. 293–304, doi: 10.1145/2348543.2348580.

[24] X. Kang, B. Huang, and G. Qi, "A novel walking detection and step counting algorithm using unconstrained smartphones," *Sensors*, vol. 18, no. 1, p. 297, Jan. 2018, doi: 10.3390/s18010297.

[25] R. Leonardo, G. Rodrigues, M. Barandas, P. Alves, R. Santos, and H. Gamboa, "Determination of the walking direction of a pedestrian from acceleration data," in *Proc. Int. Conf. Indoor Positioning Indoor Navigat. (IPIN)*, Sep. 2019, pp. 1–6, doi: 10.1109/IPIN.2019.8911801.

[26] H. Weinberg, "Using the ADXL202 in pedometer and personal navigation applications," Analog Devices, Inc., Norwood, MA, USA, Appl. Note AN-602, 2002.

[27] R. Ma, Q. Guo, C. Hu, and J. Xue, "An improved WiFi indoor positioning algorithm by weighted fusion," *Sensors*, vol. 15, no. 9, pp. 21824–21843, Aug. 2015, doi: 10.3390/s150921824.

[28] Y. Zhang, J. Ma dziuk, C. H. Quek, and B. W. Goh, "Curvature-based method for determining the number of clusters," *Inf. Sci.*, vol. 416, pp. 414—428, Nov. 2017, doi: 10.1016/j.ins.2017.05.024.

[29] M. Müller, "Dynamic time warping," in *Information Retrieval for Music and Motion*. 1st ed. Berlin, Germany: Springer, 2007, pp. 69–84, doi: 10.1007/978-3-540-74048-3_4.

[30] E. J. Keogh and M. J. Pazzani, "Derivative dynamic time warping," in *Proc. SIAM Int. Conf. Data Mining*, Apr. 2001, pp. 1–11, doi: 10.1137/1.9781611972719.1.

[31] M. Isard and A. Blake, "Visual tracking by stochastic propagation of conditional density," in *Proc. 4th Eur. Conf. Comput. Vis.*, 1996, pp. 343–356, doi: 10.1023/A:1008078328650.

[32] D. Arthur and S. Vassilvitskii, "How slow is the k-means method?" in *Proc. 22nd Annu. Symp. Comput. Geometry SCG*, 2006, pp. 144–153, doi: 10.1145/1137856.1137880.

RICARDO SANTOS received the B.S. and M.S. degrees in biomedical engineering from the Faculdade de Ciências e Tecnologia of NOVA University of Lisbon (FCT NOVA), Portugal, in 2016 and 2018, respectively, where he is currently pursuing the Ph.D. degree in biomedical engineering.

Since 2018, he has been working with the Fraunhofer Center for Assistive Information and Communication Solutions (AICOS), Portugal, primarily as a Junior Researcher until 2020, and currently as a Scientist. His research interests include indoor location field, and the development of intelligent systems with AI methods for different areas, such as medical diagnosis and prognosis.

RICARDO LEONARDO received the M.Sc. degree in biomedical engineering from the Faculdade de Ciências e Tecnologia of NOVA University of Lisbon (FCT NOVA), in 2018, where he is currently pursuing the Ph.D. degree in biomedical engineering.

He started collaborating with the Fraunhofer Center for Assistive Information and Communication Solutions (AICOS) in 2017. His research interests include indoor positioning solutions based on pervasive data sources, namely inertial data, sound, RF signals, and geomagnetism. He has since also worked on applying computer vision and deep learning to retinal images for explainable computer aided diagnosis and image quality, enhancement, and synthesis.

MARÍLIA BARANDAS received the M.S. degree in biomedical engineering from the Faculdade de Ciências e Tecnologia of NOVA University of Lisbon (FCT NOVA), in 2013, where she is currently pursuing the Ph.D. degree in biomedical engineering.

She has been working with the Fraunhofer Center for Assistive Information and Communication Solutions (AICOS) as a Scientist since 2015. Prior to joining AICOS, she was an Assistant Lecturer with the Electrical and Computer Engineering Department, FCT NOVA, and a Research Engineer with the Computational Intelligence Research Group, Centre of Technology and Systems. Her research interests include knowledge extraction, probability theory, machine learning, and explainable artificial intelligence.

DINIS MOREIRA received the M.S. degree in bioengineering from the Faculty of Engineering, University of Porto, in 2015.

He started collaborating with the Fraunhofer Center for Assistive Information and Communication Solutions (AICOS) in 2016. His research interests include fall prevention, human movement characterization, and activity recognition, based on inertial sensor data. Since then, he has been working in several projects related to pattern recognition, data mining, and machine learning.

TIAGO ROCHA received the M.S. degree in informatics and computer engineering from the Faculdade de Engenharia da Universidade do Porto (FEUP), in 2013.

He started his collaboration with the Fraunhofer Center for Assistive Information and Communication Solutions (AICOS) as a Researcher immediately after. His research interests include activity recognition, indoor positioning and navigation, namely the integration of several positioning layers to work as a single system. Since, he started working with AICOS, he also worked in several mobile development projects for Android and iOS.

PEDRO ALVES received the M.S. degree in electrical engineering and computer science from the Faculdade de Engenharia da Universidade do Porto, in 2018.

He started collaborating with the Fraunhofer Center for Assistive Information and Communication Solutions (AICOS) in 2018 on indoor positioning with a major emphasis on mobile network data. Since then, he worked with computer vision in the medical field and embedded testing.

JOÃO P. OLIVEIRA received the Ph.D. degree in electrical and computer engineering from the Instituto Superior Técnico, Engineering School, University of Lisbon, Portugal, in 2010.

He is currently a Researcher with the Software System Engineering Group, Information Sciences, Technologies and Architecture Research Center (ISTAR-IUL) and with the Pattern and Image Analysis Group, Instituto de Telecomunicacoes, Lisbon, Portugal. He is also an Assistant Professor with the Department of Information Science and Technology, Instituto Universitario de Lisboa (ISCTE-IUL). His current research interests include signal and image processing, and machine learning.

HUGO GAMBOA (Senior Member, IEEE) received the Ph.D. degree in electrical and computer engineering from the Instituto Superior Técnico of University of Lisbon (IST UL), in 2007.

He co-founded and is the President of PLUX, a company that develops biosignals monitoring wearable technology. He has been a Senior Researcher with the Fraunhofer Center for Assistive Information and Communication Solutions (AICOS) since 2014. He is currently a Researcher with the Laboratory for Instrumentation, Biomedical Engineering and Radiation Physics (LIBPhys), Faculdade de Ciências e Tecnologia of NOVA University of Lisbon (FCT NOVA), where he is also an Assistant Professor with the Physics Department. His research interests include biosignals processing and instrumentation.

∙ ∙ ∙